Atom Indonesia

Journal homepage: http://atomindonesia.brin.go.id

# Internal Conversion and Internal Pair Production, Need for New Measurements

**S. Sarfarazi, M. Sohani***

*Faculty of Physics, Shahrood University of Technology, Shahrood 3619995161, Iran*

**ARTICLE INFO**

*Article history:*
Received 18 November 2024
Received in revised form 17 August 2025
Accepted 18 December 2025

*Keywords:*

Internal Conversion (IC)
Internal Pair Production (IPP)
Internal Conversion Coefficient (ICC)
E0 transition

**ABSTRACT**

The study and spectroscopy of Internal Conversion (IC) and Internal Pair Production (IPP) processes provide valuable information about nuclei and nuclear states. In the present work, Internal Conversion and Internal Pair Production processes are initially reviewed. Then, the theoretical and experimental IC coefficients, as well as the theoretical and experimental ratio of IC to IPP probabilities for the E0 transition in several isotopes are compiled and compared. The relative differences between theoretical and experimental coefficients are obtained. Significant discrepancies are observed between theoretical and experimental coefficients for several isotopes such as $^{101}$Ru, $^{152}$Gd, $^{58}$Co, $^{125}$Te, and other isotopes. These comparisons and the relative differences reveal the need for more accurate experimental measurements and improved theoretical models.



## INTRODUCTION

Gamma decay, Internal Conversion (IC), and Internal Pair Production (IPP) are processes for the electromagnetic deexcitation of excited nuclei. The IPP process may occur when excitation energy is at least 1.022 MeV (twice the rest mass energy of the electron). Additionally, in cases of transitions such as $0^+ \rightarrow 0^+$ where γ emission is forbidden by angular momentum and parity conservation, IC, IPP, and double photon emission are the available processes [1]. The study of IC and IPP processes offers significant information about nuclei and nuclear states [2]. Experimental measurements and theoretical calculations have been performed in both cases. Various methods and instruments are employed to measure IC and IPP coefficients [3-9]. Experimental results on both ICC and IPP coefficients suffer from relatively large experimental standard errors in several isotopes, due to complicated decay schemes, low signal-to-noise ratios in the detection setup, or the coexistence of other radioisotopes.

*Corresponding author.
E-mail address: Sohani@shahroodut.ac.ir
DOI: https://doi.org/10.55981/aij.2026.1557

There are several models which are calculating the IC and IPP coefficients for these isotopes using different methods, assumptions, and approximations. As a result, in several isotopes, there are not a well agreement between experimental values and calculated ones. Therefore, favoring one model to describe IC and IPP processes is challenging.

In the present work, IC and IPP processes are initially reviewed. Then, the experimental and theoretical results of IC and IPP coefficients of several isotopes are compiled and compared. In some isotopes, the need for more precise measurements and improved theoretical models is apparent.

## THEORY

### Internal conversion

Internal conversion is an electromagnetic process by which the excitation energy of nuclei results in the emission of an atomic electron. Internal conversion measurement can be used to: i) study nuclear structure and decay scheme, ii) determine transition multipolarity, and iii) assign spin and parity of nuclear states [10]. In general,

the Internal Conversion Coefficient (ICC) is defined as Eq. (1) [11]:

$$\alpha_i=\frac{\lambda_i}{\lambda_\gamma} \qquad i=K, L, M, N, \tag{1}$$

Where $\lambda_i$ is the probability of i$^{th}$-conversion electron emission, where $i$ is the atomic shell, and $\lambda_\gamma$ is the probability of the γ emission. Internal conversion in cases where single gamma emission is forbidden (E0 transitions) is reviewed in the following sections.

ICCs can be obtained both theoretically and experimentally. Theoretical calculation of ICC is based on quantum mechanics theory and usually is in the framework of the first-order perturbation. The main methods for ICC calculation include relativistic Hartree-Fock-Slater (RHFS) and Dirac-Fock (DF). There are many attempts to calculate ICCs that are presented as ICC tables. Over the years, ICC tables for different atomic shells, atomic number ranges, nuclear models, and atomic field models have been published. The tables contain different approximations about exchange interactions between atomic electrons, consideration of holes (electron vacancies created in the atomic shell due to the internal conversion process), and so on [10,12-16]. The most widely used ICC tables are obtained by Hager and Seltzer (1968) denotes as HS [14], Rosel et al. (1978) denotes as RFAP [15], Band and Trzhaskovskaya 1978) denotes as BT, Band et al. (2002) denotes as BTNTR [16], and Raman et al. (2002) denotes as RNIT [10]. The HS, RFAP, and BT tables are based on the RHFS method, while the BTNTR and RNIT use the DF method. In the RHFS method, the exchange interaction is considered through applying an approximation, whereas in the DF method, it is taken into account exactly.

An important subject in ICC calculation is the relationship between the time scale for filling the atomic hole and the time required for the conversion electron to escape the atom. Consideration of the atomic hole in ICC calculations involves two approaches: i) the hole is assumed to be filled instantaneously, or ii) it is assumed to remain unfilled for the duration of the conversion electron removal from the atom. The hole is taken into account in the HS, BT, and RNIT tables and is neglected in the RFAP and BTNTR tables. Considering the hole in ICC calculation, the electron wave function for the initial state (bound) should be calculated in the Self-Consistent Field (SCF) of the neutral atom, while the electron wave function for the final state (continuum) is calculated in the SCF of the positive ion. Therefore, when both bound and continuum wave functions are calculated in the SCF of a neutral atom, the presence of the hole is neglected. There is a second approach to account for the atomic hole in ICC calculations, known as the frozen orbital approximation. In this method, the continuum wavefunctions are calculated in the field of the ion, where the field is not SCF and is constructed using the bound wavefunctions of a neutral atom. The RNIT table provides a second set of calculations using frozen orbital approximation as well. In the following sections, the K-conversion coefficient is reviewed in several isotopes for which the theoretical and corresponding experimental ICCs are available.

## Internal Pair Production (IPP)

Internal Pair production (IPP) is another process to deexcite highly excited nuclei (more than 1.022 MeV). IPP coefficient is defined as Eq. (2) [11].

$$\alpha_p=\frac{\lambda_p}{\lambda_\gamma} \tag{2}$$

Where $\lambda_p$ is the probability of electron-positron pair emission, and $\lambda_\gamma$ is the probability of photon emission. The IPP process is important, especially in electric monopole (E0) transitions. Single gamma emission is forbidden in the E0 transition; therefore, this transition proceeds via IC, IPP, and double photon emission processes. Since the probability of the double photon emission is very low, it is neglected in calculations. E0 transition probability, $W(E0)$, can be expressed as Eq. (3) [11].

$$W(E0)=W_{IC}(E0)+W_{IPP}(E0) \tag{3}$$

Where $W_{IC}(E0)$ and $W_{IPP}(E0)$ are the probabilities of transition for IC and IPP, respectively. For knowledge of the characteristics of the E0 transition, an understanding of the electronic factor is necessary. E0 transition probability can be expressed as nuclear ($\rho(E0)$) and atomic ($\Omega(E0)$) components as Eq. (4).

$$W_i(E0)=|\rho(E0)|^2.\Omega_i(E0) \tag{4}$$

Where $\rho(E0)$ is the monopole transition strength parameter, $\Omega_i(E0)$ is the electronic factor, and $i$ refers to the i$^{th}$-conversion or internal pair production process.

There are rare theoretical calculations for $\Omega_{IPP}(E0)$, including those by Lombard et al. (1968) denotes as LPB [17], Passoja and Salonen (1986) denotes as PS [18], Soff et al. (1981) denotes as SSG [19], and Dowie et al. (2020) denotes as DKES [20] calculations. The LPB calculation includes an exact calculation using relativistic electron wavefunctions for point like nucleus. The PS calculation uses the Born approximation with corrections for the nuclear

Coulomb effect, also considering a point-like nucleus. The SSG calculation uses relativistic wavefunctions for electron and positron, considering the finite size of the nucleus. The DKES calculation considers the nuclear Coulomb effect but does not take into account the finite size of the nucleus. The effect of atomic screening is considered in DKES, whereas it is omitted in other models. In the following sections, the ratio of K-conversion to internal pair production probability (IPP coefficient) for the E0 transition is reviewed for several isotopes.

## RESULTS AND DISCUSSION

### Theoretical and experimental internal conversion coefficients

Tables 1-4 present the experimental and five theoretical values of $\alpha_k$, derived from aforementioned tables, for several isotopes corresponding to the E2, E3, M3, and M4 transitions, respectively [10]. For some isotopes, new experimental measurements have been carried out, which are reported in Tables 2 and 4 [5,21,22]. To compare the theoretical and experimental ICCs, the relative differences between the theoretical values from each table and the experimental value for various isotopes have been obtained as Eq. (5)

$$\Delta = \frac{|theoretical\ value - experimental\ value|}{experimental\ value} \quad (5)$$

Then the relative differences ($\Delta$) for each isotope are plotted in Fig. 1 for E2, E3, M3, and M4 transitions. The results based on the HS, RFAP, BT, BTNTR, and RNIT tables are shown by the symbols □, ○, △, ▽, ◇, respectively.

**Table 1.** Theoretical and experimental K-conversion coefficients ($\alpha_k$) in E2 transition [10].

| Isotope | Transition energy (keV) | Transition Half-life | Experimental value | Theoretical value (HS) | Theoretical value (RFAP) | Theoretical value (BT) | Theoretical value (BTNTR) | Theoretical value (RNIT) |
|---|---|---|---|---|---|---|---|---|
| $^{54}$Cr | 834.855 *3* | 7.9ps | 0.000224 *10** | - | - | 0.0002233 | 0.0002220 | 0.0002218 |
| $^{58}$Fe | 810.764 *15* | 6.54ps | 0.00030 *1* | - | - | 0.0003012 | 0.0002996 | 0.0002994 |
| $^{60}$Ni | 1173.251 *4* | 0.30ps | 0.000150 *6* | - | - | 0.0001508 | 0.0001502 | 0.0001500 |
| $^{101}$Ru | 324.8 *2* | 0.20ns | 0.0160 *8* | 0.01781 | 0.0179 | 0.01786 | 0.01761 | 0.01768 |
| $^{152}$Sm | 121.782 *1* | 1.428ns | 0.669 *8* | 0.6848 | 0.676 | 0.6862 | 0.6646 | 0.6781 |
| $^{152}$Gd | 344.282 *2* | 31.9ps | 0.0286 *8* | 0.03111 | 0.0311 | 0.03123 | 0.03081 | 0.03102 |
| $^{154}$Gd | 123.071 *2* | 1.186ns | 0.634 *16* | 0.6623 | 0.653 | 0.6637 | 0.6421 | 0.6557 |
| $^{160}$Dy | 86.788 *1* | 2.02ns | 1.53 *6* | 1.585 | 1.55 | 1.592 | 1.513 | 1.565 |
| $^{166}$Er | 80.577 *7* | 1.82ns | 1.67 *5* | 1.706 | 1.65 | 1.704 | 1.606 | 1.671 |
| $^{170}$Yb | 84.255 *1* | 1.60ns | 1.40 *4* | 1.437 | 1.39 | 1.434 | 1.352 | 1.406 |
| $^{198}$Hg | 411.805 *2* | 23.16ps | 0.0298 *3* | 0.03014 | 0.0302 | 0.03017 | 0.02974 | 0.02997 |
| $^{200}$Hg | 367.944 *10* | 46.4ps | 0.0397 *8* | 0.03913 | 0.0391 | 0.03912 | 0.03848 | 0.03883 |
| $^{207}$Pb | 569.703 *2* | 130.5ps | 0.0157 *5* | 0.01590 | 0.0160 | 0.01592 | 0.01575 | 0.01583 |

*0.000224 *10* ≡ 0.000224±0.000010

**Table 2.** Theoretical and experimental K-conversion coefficients ($\alpha_k$) in E3 transition [10].

| Isotope | Transition energy (keV) | Transition Half-life | Experimental value | Theoretical value (HS) | Theoretical value (RFAP) | Theoretical value (BT) | Theoretical value (BTNTR) | Theoretical value (RNIT) |
|---|---|---|---|---|---|---|---|---|
| $^{75}$As | 303.925 *2* | 16.79ms | 0.0472 *23*<br>0.045 *2* [a] | 0.04701 | 0.0471 | 0.04730 | 0.04663 | 0.04694 |
| $^{83}$Kr | 32.147 *2* | 1.83h | 454 *15* | 495.9 | 477 | 494.9 | 458.1 | 483.1 |
| $^{103}$Rh | 39.756 *6* | 56.12m | 136 *6*<br>141.1 *23* [b] | 139.4 | 133 | 138.8 | 127.3 | 135.1 |
| $^{107}$Ag | 93.13 *2* | 44.3s | 9.2 *4* | 9.391 | 9.23 | 9.397 | 9.034 | 9.273 |
| $^{109}$Ag | 88.034 *2* | 39.6s | 11.3 *3* | 11.56 | 11.3 | 11.57 | 11.10 | 11.41 |
| $^{134}$Cs | 127.502 *3* | 2.91h | 2.60 *4*<br>2.742 *15* [c] | 2.771 | 2.73 | 2.775 | 2.677 | 2.741 |

**Table 3.** Theoretical and experimental K-conversion coefficients ($\alpha_k$) in M3 transition [10].

| Isotope | Transition energy (keV) | Transition Half-life | Experimental value | Theoretical value (HS) | Theoretical value (RFAP) | Theoretical value (BT) | Theoretical value (BTNTR) | Theoretical value (RNIT) |
|---|---|---|---|---|---|---|---|---|
| $^{58}$Co | 24.889 *21* | 9.15h | 2030 *90* | - | - | 1894 | 1753 | 1839 |
| $^{60}$Co | 58.59 *1* | 10.47m | 41.2 *18* | - | - | 40.16 | 38.41 | 39.33 |
| $^{94}$Nb | 40.902 *12* | 6.263m | 750 *37* | 783.8 | 781 | 786.5 | 730.7 | 765.8 |

**Table 4.** Theoretical and experimental K-conversion coefficients ($\alpha_k$) in M4 transition [10].

| Isotope | Transition energy (keV) | Transition Half-life | Experimental value | Theoretical value (HS) | Theoretical value (RFAP) | Theoretical value (BT) | Theoretical value (BTNTR) | Theoretical value (RNIT) |
|---|---|---|---|---|---|---|---|---|
| $^{85}$Kr | 304.871 *20* | 4.480h | 0.432 *20* | 0.4365 | 0.438 | 0.4390 | 0.4293 | 0.4337 |
| $^{87}$Sr | 388.532 *3* | 2.803h | 0.175 *6* | 0.1824 | 0.183 | 0.1833 | 0.1796 | 0.1813 |
| $^{90}$Y | 479.50 *5* | 3.19h | 0.0856 *29* | 0.08288 | 0.0834 | 0.08335 | 0.08186 | 0.08249 |
| $^{101}$Rh | 157.32 *4* | 4.34d | 21.2 *10* | 21.38 | 21.3 | 21.51 | 20.67 | 21.13 |
| $^{113}$In | 391.691 *8* | 1.6582h | 0.438 *7* | 0.4484 | 0.449 | 0.4505 | 0.4384 | 0.4437 |
| $^{117}$Sn | 156.02 *3* | 13.60d | 30.2 *15* | 31.63 | 31.4 | 31.78 | 30.40 | 31.12 |
| $^{119}$Sn | 65.66 *1* | 293.1d | 1700 *80*<br>1621 *25* [c] | 1661 | 1620 | 1668 | 1543 | 1618 |
| $^{125}$Te | 109.276 *15* | 57.40d | 167 *7*<br>185.0 *40* [c] | 188.6 | 186 | 189.7 | 179.4 | 185.1 |
| $^{127}$Te | 88.26 *8* | 109d | 484 *23*<br>484 *6* [c] | 497.2 | 487 | 498.9 | 467.6 | 485.3 |
| $^{129}$Xe | 196.56 *3* | 8.88d | 13.61 *67* | 13.92 | 13.8 | 13.94 | 13.37 | 13.66 |
| $^{137}$Ba | 661.660 *3* | 2.552m | 0.0902 *8*<br>0.0915 *5* [c] | 0.09261 | 0.0929 | 0.09289 | 0.09067 | 0.09148 |
| $^{193}$Ir | 80.22 *2* | 10.53d | 104 *3*<br>103.0 *8* [c] | 110.3 | 103 | 107.9 | 91.93 | 103.2 |
| $^{197}$Pt | 346.5 *2* | 95.41m | 4.02 *8*<br>4.23 *7* [c] | 4.401 | 4.38 | 4.344 | 4.187 | 4.272 |
| $^{197}$Hg | 164.97 *7* | 23.8h | 73.9 *8* | 77.05 | 76.0 | 76.08 | 71.69 | 74.26 |
| $^{207}$Pb | 1063.662 *4* | 0.805s | 0.0945 *22* | 0.09695 | 0.0977 | 0.09491 | 0.09338 | 0.09427 |

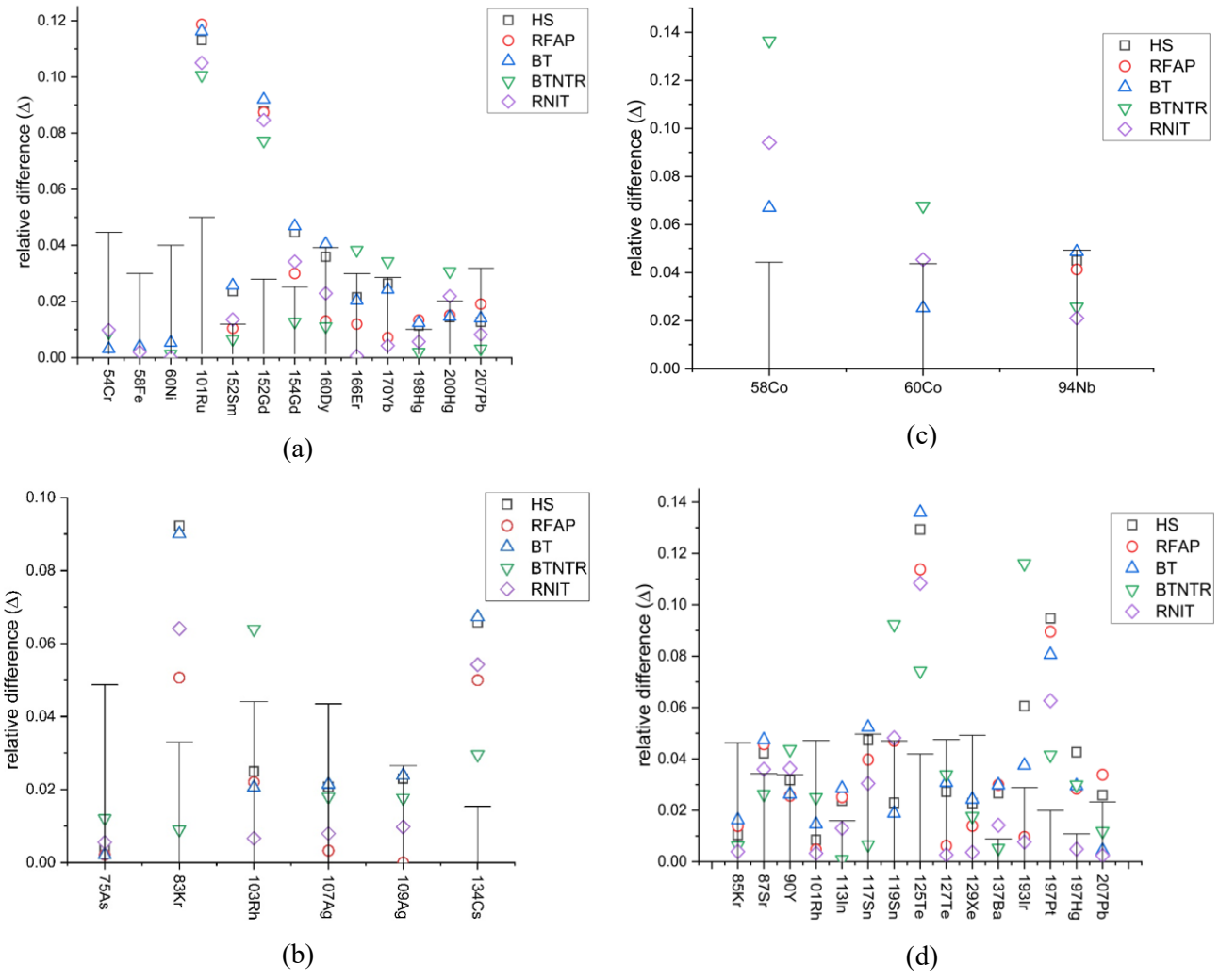


**Fig. 1.** The relative differences (Δ) between theoretical and experimental values for $\alpha_k$ as $\frac{|\alpha_{k,th.}-\alpha_{k,ex.}|}{\alpha_{k,ex.}}$ in a) E2, b) E3, c) M3, and d) M4 transitions for several isotopes.

Comparing the experimental values and calculated ones for ICCs shown in Fig. 1, the magnitude of the experimental standard error, together with the relative location of the Δ points with respect to error bar, provides a basis for evaluating the agreement between theory and experiment. It is observed that: i) In most cases, there are significant experimental standard errors, for these isotopes one can improve the experimental accuracy, both on statistics and systematics., ii) In isotopes such as $^{101}$Ru, $^{152}$Gd, $^{58}$Co and $^{125}$Te the relative differences between theoretical and experimental values are considerable, while theoretical values are close together. For these isotopes one needs to a more realistic models by considering higher order effects such as taking into account vacuum polarization and electron correlation corrections, nuclear deformation and atomic effects., iii). In isotopes such as $^{60}$Ni, $^{75}$As, $^{94}$Nb and $^{85}$Kr, all theoretical values lie within the range of the experimental standard errors. This implies that the accuracy of the experimental data should be enhanced to discriminate between theoretical models and allow selection of a more reliable one., iv) For some isotopes such as $^{134}$Cs, $^{197}$Pt, all theoretical values are outside the range of the experimental standard errors, while in others such as $^{83}$Kr, $^{154}$Gd,$^{193}$Ir, only one or a few theoretical values lie within this range pointing to that both theory and experiment may require further improvement. As a result, for most isotopes, more accurate measurements and improved calculation methods are required. More accurate measurements have been performed for $^{75}$As, $^{103}$Rh, $^{134}$Cs, $^{119}$Sn, $^{125}$Te, $^{127}$Te, $^{137}$Ba, $^{193}$Ir, and $^{197}$Pt isotopes [5,21,22]. The relative differences between theoretical and experimental values using old and new experimental values are plotted in Fig. 2. As seen in Fig. 2, the accuracy of new measurement for $^{137}$Ba has significantly improved. In this case, only one Δ point, based on the RNIT model, lies within the experimental standard error. Therefore, RNIT can be selected as the superior theoretical model, as it shows the closest agreement with experimental value. However, in all cases, the experimental standard errors and relative differences are decreased in the new data, and in most cases, the theoretical values from the RNIT table show better agreement with experiments. Accordingly, one can conclude that the DF method performs better than the RHFS method.

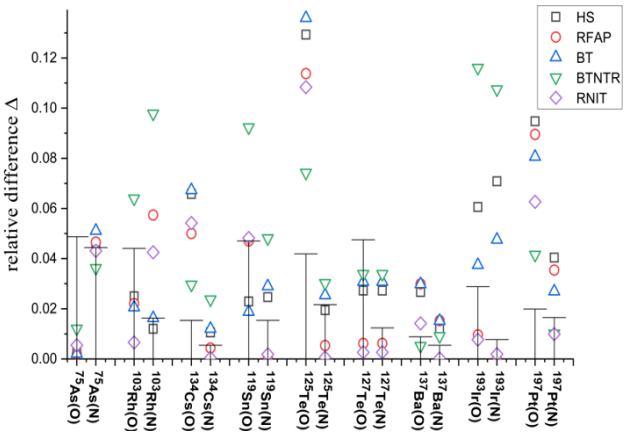


**Fig. 2.** The relative differences (Δ) between theoretical and experimental values for $\alpha_k$ as $\frac{|\alpha_{k,th.}-\alpha_{k,ex.}|}{\alpha_{k,ex.}}$ using two experimental values. N represents the new value, and O represent old value.

The difference between these methods lies in their treatment of the exchange interaction between bound electrons, as well as between bound and ejected electrons. Since the RNIT model gives the best overall agreement, accounting for the exact exchange interactions in the calculation of both bound and continuum wavefunctions may lead to more accurate results. Furthermore, considering the presence of the atomic hole in ICC calculations seems to be important. Performing more accurate measurements for other isotopes will be useful.

## Internal pair production in E0 transition

Theoretical and experimental ratios of K-conversion to IPP probabilities for the E0 transition in several isotopes are listed in Table 5. The relative differences between each theoretical value and experimental value are obtained according to Eq. 5. Due to the inherently low probability of IPP occurring during nuclear transitions, measuring this process can be challenging. In contrast to isotopes such as $^{90}$Zr, which undergo only IPP and IC, in the cases such as $^{42}$Ca where a competing gamma-ray emission process exists, the difficulty of this measurement increases. Additionally, positron detection is problematic owing to the fact that positrons annihilate easily. Therefore, it is preferable to employ annihilation-photon detection methods or to utilize an MOS setup in vacuum for in- and off-line measurements. Figure 3 shows the relative differences for each isotope of table 5; where the results from LPB, PS, SSG, and DKES calculations are shown by the symbols □, ○, △ and ▽, respectively.

**Table. 5.** Theoretical and experimental ratio of IC to IPP probability in E0 transition [19].

| isotope | Transition energy (keV) | Transition half-life | Experimental value | Theoretical value (LPB) | Theoretical value (PS) | Theoretical value (SSG) | Theoretical value (DKES) |
|---|---|---|---|---|---|---|---|
| $^{16}$O | 6048.2 | 67ps | $(4.00\pm0.46)\times10^{-5}$ | $3.92\times10^{-5}$ | $3.82\times10^{-5}$ | $3.8\times10^{-5}$ | $3.45\times10^{-5}$ |
| $^{40}$Ca | 3352.6 | 2.16ns | $(6.94\pm0.20)\times10^{-3}$ | $6.0\times10^{-3}$ | $7.16\times10^{-3}$ | $7.16\times10^{-3}$ | $6.86\times10^{-3}$ |
| $^{42}$Ca | 1837.3 | 387ps | 0.111 *22* | 0.072 | 0.139 | 0.139 | 0.133 |
| $^{54}$Fe | 2561.3 | ≥1.4ps | 0.053 *3* | - | 0.0598 | - | 0.0575 |
| $^{60}$Ni | 2284.87 | >1.5ps | 0.130 *28* | - | 0.135 | - | 0.135 |
| $^{64}$Zn | 1910 | 0.95ns | 0.46 *7* | - | 0.472 | - | 0.475 |
| $^{70}$Ge | 2307.1 | ≤40ps | 0.20 *8* | - | 0.212 | - | 0.207 |
| $^{90}$Zr | 1760.70 | 61.3ns | 3.0 *11*<br>2.38 *8*<br>2.28 *32* | 1.42 | 2.48 | 2.52 | 2.48 |

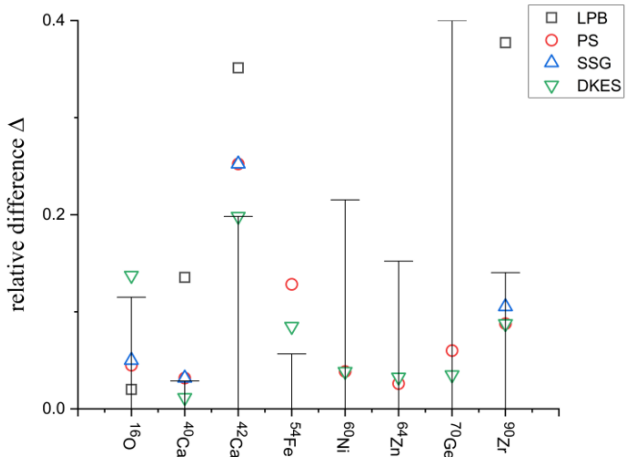


**Fig. 3.** The relative differences (Δ) between theoretical and experimental ratio of K-conversion to IPP probability as $\frac{|\text{theoretical value-experimental value}|}{\text{experimental value}}$ in E0 transition.

As shown in Fig. 3, in all cases except for $^{40}$Ca, there are significant experimental standard errors. In $^{42}$Ca and $^{54}$Fe, all theoretical values lie outside the range of the experimental standard error, whereas for isotopes such as $^{60}$Ni, $^{64}$Zn, and $^{70}$Ge the theoretical values lie within the range of the experimental standard error. In most cases, the DKES model shows better agreement with the experimental value compared to other theoretical models. Among the theoretical models introduced earlier, only DKES includes the atomic screening effect. These results suggest that the inclusion of the screening effect plays an important role in improving the accuracy of the theoretical calculations. Therefore, similar to the IC process, there is apparent need for more precise measurements and improved theoretical IPP calculations.

## CONCLUSION

The IC and IPP processes are known as important processes for the assignment of nuclear properties. In this study, we have reviewed the ICCs and the ratios of IC to IPP probability for E0 transitions. From the comparisons performed in the present work, significant experimental standard errors and relative differences between theoretical and experimental coefficients are observed in the IC process for isotopes such as $^{101}$Ru, $^{152}$Gd, $^{83}$Kr, $^{58}$Co, and $^{125}$Te (see Fig. 1), as well as in the IPP process for isotopes such as $^{42}$Ca and $^{70}$Ge (see Fig. 3). Furthermore, in different isotopes, the best agreement with experimental results has not been achieved through any specific calculation method.

Notably, the deformation parameter has not been considered in any of the theoretical methods. Does considering this parameter in deformed nuclei contribute to the improvement of the theoretical methods? Nuclear deformation induces an electric quadrupole moment to the electric field of nucleus, which modifies the atomic potential and consequently affects the atomic states. These modifications might have implications for theoretical models.

It is observed (see Fig. 2) that with more precise measurements, both the experimental standard errors and the agreement between theoretical and experimental values improve. Additionally, in most cases, the theoretical values based on the RNIT table show better agreement with experimental results.

The findings of this study suggest a compelling need for more precise measurements. Experimental measurements can be performed in-line or off-line. Off-line measurements are appropriate for long-lived isotopes. Given the ability of magnetic materials to generate a relatively strong magnetic field, the Mini-Orange Spectrometer [23] is well-suited for off-line measurements of long-lived isotopes such as $^{90}$Zr.

## ACKNOWLEDGMENT

This work is a part of Ph.D. Thesis of Sonia Sarfarazi under support of Faculty of Physics at Shahrood University of Technology, Iran.

## AUTHOR CONTRIBUTION

S. Sarfarazi and M. Sohani equally contributed as the main contributors of this paper. All authors read and approved the final version of the paper.

## REFERENCES


1. O. Dragoun, Adv. Electron. Electron Phys. **60** (1983) 1.
2. F. C. Zawislak, J. D. Rogers, and E. A. Meneses, Nucl. Phys. A. **211** (1973) 581.
3. M. E. Rose, G. H. Goertzel, B. I. Spinrad *et al.*, Phys. Rev. **83** (1951) 79.
4. M. Rysavy and O. Dragoun, At. Data Nucl. Data Tables. **78** (2001) 129.
5. J. C. Hardy, N. Nica, V. E. Iacob *et al.*, Appl. Radiat. Isot. **134** (2018) 406.
6. W. R. Mills, Absolute Measurments of Internal Conversion Coefficients, Ph.D. Thesis, California Institute of Technology, 1955.
7. M. Nessin, T. H. Kruse, and K. E. Eklund, Phys. Rev. **125** (1962) 639.
8. A. Passoja, R. Julin, J. Kantele *et al.,* Nucl. Phys. A. **363** (1981) 399.
9. I. Kambali, H. Suryanto, and Parwanto, Atom Indones. **42** (2016) 1.
10. S. Raman, C. W. Nestor, A. Ichihara *et al*., Phys. Rev. C. **66** (2002) 044312.
11. T. Kibedi, T. W. Burrows, M. B. Trzhaskovskaya *et al.*, Nucl. Instrum. Methods Phys. Res. A, **589** (2008) 202.
12. O. Dragoun, Z. Plajner, and F. Schmutzler, Nucl. Data Tables A. **9** (1971) 119.
13. V. F. Trusov, Nucl. Data Tables. **10** (1972) 477.
14. R. S. Hager and E. C. Seltzer, Nucl. Data Sheet Sect. A, **4** (1968) 1.
15. F. Rosel, H. M. Fries, K. Alder *et al*., At. Data Nucl. Data Tables **21** (1978) 291.
16. I. M. Band, M. B. Trzhaskovskaya, C. W. Nestor *et al*., At. Data Nucl. Data, **81** (2002) 1.
17. R. J. Lombard, C. F. Perdrisat, and J. H. Brunner, Nucl. Phys. A. **110** (1968) 41.
18. A. Passoja and T. Salonen, Electronic Factors for K-Shell-Electron Conversion Probability and Electron-Positron Pair Formation Probability in Electric Monopole Transitions, JYFL RR-2/86, 1986.
19. G. Soff, P. Schluter, and W. Greiner, Z. Phys. A. **303** (1981) 189
20. J. T. H. Dowie, T. Kibedi, T. K. Eriksen *et al.*, At. Data Nucl. Data Tables **131** (2020) 101283.
21. D. R. Rao, K. V. Sai, M. Sainath *et al*., Eur. Phys. J. A. **26** (2005) 41.
22. N. Nica, J. C. Hardy, V. E. Iacob *et al*., Phys. Rev. C. **98** (2018) 054321.
23. M. Sainath, K. V. Sai, R. Dwarakarani *et al.,* J. Nucl. Phy. Mat. Sci. Rad. A. **8** (2020) 25.